**Title:** Compartment model analysis of intravenous contrast-enhanced dynamic computed tomography in hepatic hemodynamics: a validation study using intra-arterial contrast-enhanced computed tomography

**Authors:**

Daisuke Komatsu[1)], Akira Yamada[1)], Takeshi Suzuki[1)], Masahiro Kurozumi[1)], Yasunari Fujinaga[1)], Kazuhiko Ueda[2)], Masumi Kadoya[1)]

**Affiliations:**

1) Department of Radiology, Shinshu University School of Medicine

2) Diagnostic Imaging Center, The Canter Institute Hospital of Japanese Foundation for Cancer Research

**Corresponding author:**

Akira Yamada, MD, PhD

Department of Radiology, Shinshu University School of Medicine

3-1-1 Asahi, Matsumoto, Nagano 390-8621, Japan

E-mail: a_yamada@shinshu-u.ac.jp

Tel: +81-263-37-2650

Fax: +81-263-37-3087

**Running Title:**

Validation of hepatic CT perfusion study

**Abstract**

*Aim:* To verify the utility of the 2-in-1-out-compartment model analysis (CMA) of intravenous contrast-enhanced dynamic computed tomography (IV-CT) for evaluating hepatic arterial and portal venous flow using intra-arterial contrast-enhanced CT (IA-CT).

*Methods:* We retrospectively evaluated 49 consecutive patients who underwent IV-CT and were radiologically or histologically diagnosed as having hepatic malignant lesion (51 classical hepatocellular carcinomas [HCC], 4 early HCC, 3 cholangiolocellular carcinomas, 1 mixed HCC, 3 cholangiocellular carcinomas). As a gold standard for hepatic arterial and portal blood flows, we defined the normalized enhancement in CT values on CTAP (nCTAP) and CTHA (nCTHA). The hepatic arterial ($k_{1a}$) and portal venous inflow velocity ($k_{1p}$) constants in hepatic lesions and surrounding liver parenchyma were obtained from the CMA of IV-CT with various outflow velocity constant ($k_2$) limits using the nonlinear least square method. The correlation coefficient between the normalized enhancement in IA-CT and CMA of IV-CT was statistically evaluated according to various $k_2$ limits.

*Results:* The highest mean correlation coefficient between $k_{1a}$ and nCTHA (r=0.65, P<0.0001) was observed when $k_2 \leqq 0.035$. The highest mean correlation coefficient between $k_{1p}$ and nCTAP (r=0.69, P<0.0001) was observed when $k_2 \leqq 0.045$. The decrease in correlation coefficient was significant when the upper $k_2$ limit was lower than 0.03 or higher than 0.07 compared to the best mean correlation coefficient (P < 0.05).

*Conclusion:* Hepatic arterial and portal venous flows can be evaluated quantitatively to some extent with appropriate outflow velocity constant limits using the CMA of IV-CT.

**Key words:**

Computed tomogramphy, Liver, Perfusion imaging, Hepatic artery, Portal vein

## Introduction

Evaluation of portal blood flow is important for the diagnosis and treatment of hepatocellular carcinoma (HCC), because portal blood flow in HCC is reduced as the grade of malignancy increases [1]. However, portal blood flow cannot be evaluated separately and independently by intravenous contrast-enhanced computed tomography (IV-CT) that is commonly used in clinical practice [1].

In contrast, intra-arterial contrast-enhanced CT (IA-CT), such as CT during arterioportography (CTAP) and CT during hepatic arteriography (CTHA), has been regarded as the gold standard for evaluating liver hemodynamics [1-5], because arterial and portal blood flows can be separated physiologically. However, this technique is invasive [2,3].

Therefore, liver perfusion study using IV-CT has been proposed in clinical practice, because arterial and portal blood flows can be separated by computation without invasive procedures. Various useful tissue hemodynamic parameters can be quantitatively obtained from a CT perfusion study. Several studies have shown that the parameters obtained from a CT perfusion study correlate well with the presence and range of tumor vessels [6-8]. Although CT perfusion studies are known to be useful in the

assessment of hepatic perfusion associated with disease severity in patients with chronic liver disease [9,10], earlier detection of liver malignancies [8], and evaluation of treatment effects in HCC [11,12], no validation study has been conducted to date between IA-CT and a liver perfusion study using IV-CT.

Furthermore, the 2-in-1-out-compartment model analysis (CMA) has been adapted to study liver perfusion [13-15]. The movement of the contrast medium between pharmacokinetic compartments in the liver can be expressed using quantitative parameters, such as the arterial inflow velocity constant ($k_{1a}$), portal venous inflow velocity constant ($k_{1p}$), and venous outflow constant ($k_2$), in this model. Because the CMA in liver perfusion is more complex than the 1-in-1-out-compartment model used in other non-hepatic tissues, the parameters should be determined by non-linear procedures such as curve fitting of the time-density curve (TDC) using the non-linear least square method [16,17]. Appropriate limits for perfusion parameters should be determined in these procedures to avoid a local minima problem that could cause the computation to stop at an unreasonable answer because of false-best curve fitting [18]. However, details regarding this procedure have not been verified in comparison to the arterial and portal venous flows observed by IA-CT.

Therefore, the purpose of this study was to verify the utility of the CMA of IV-CT for evaluating hepatic arterial and portal venous flows in comparison to IA-CT with special emphasis on parameter limits during curve-fitting procedures.

## Methods

### Patient characteristics

This retrospective study was approved by the Institutional Review Board of Shinshu University School of Medicine (Matsumoto, Japan), and informed consent was obtained from all patients included in this study. We included 38 consecutive patients (25 men and 13 women; mean age, 74 years) who were radiologically diagnosed as having classical HCC and underwent both IV-CT and IA-CT (CTAP and CTHA) within 30 days as part of the preoperative evaluation for surgical resection or transarterial chemoembolization between 2008 and 2013 at our hospital. Seven patients had hepatitis B virus infection, 19 had hepatitis C virus infection, one had both hepatitis B and C virus infection, two had alcoholic or non-alcoholic steatohepatitis, one had primary biliary cirrhosis, and eight had neither hepatitis B nor hepatitis C liver cirrhosis. Eventually, 51 HCCs radiologically diagnosed using IA-CT (decreased portal venous

flow on CTAP, and increased arterial flow, washout, corona, and capsular enhancement on CTHA) with a maximum diameter of more than 2 cm (mean, 2.4 cm) in the patients were evaluated in this study. Additionally, 11 consecutive patients (7 men and 11 women; mean age, 70 years) who were histologically diagnosed as having other hepatic malignant lesions including 4 early HCCs (eHCC), 3 cholangiolocellular carcinomas (CoCC), 1 mixed HCC, and 3 cholangiocellular carcionomas (CCC) were included in this study according to the same inclusion criteria as the patients with HCC. In overall 49 patients, 19, 22, and 8 were diagnosed as cirrhosis, chronic hepatitis, and normal liver clinically or histologically if available.

IA-CT protocol

CTAP and CTHA were performed using Aquilion 16 (TOSHIBA Medical Systems, Ootawara, Japan) in the angiography room. All the patients underwent single phasic CTAP first and 2 to 3 phasic CTHA.

In the CTAP scan, 5 μg of prostaglandin E1 (Liple; Mitsubishi Tanabe Pharma Corporation, Osaka, Japan) was injected into the superior mesenteric artery immediately before the injection of contrast medium. CTAP scanning began 30 s after the injection

of an infusion of 300 mgI/mL iodine contrast agent (Omnipaque; Daiichi Sankyo, Tokyo, Japan) (50 mL) + saline (25 mL) at 1.8 mL/s through a catheter placed in the superior mesenteric artery. CTAP images were acquired for 1-mm-thick sections including the whole liver.

The first phase of CTHA scanning began 10 s after starting the injection of 300 mgI/mL iodine contrast agent (Omnipaque; Daiichi Sankyo) (30 mL) at 1 mL/s through a catheter placed in the common or proper hepatic artery. The infusion was continued throughout scanning. The second and the third phase scanning began 30 s after the end of contrast agent infusion and 30 s after the end of second phase scanning. All phase of CTHA images were acquired for 1-mm-thick sections including the whole liver.

Image analysis of IA-CT (CTAP and CTHA)

Four regions of interest (ROIs) were located at the hepatic artery, portal vein, liver, and hepatic malignant lesions manually on the IA-CT images by board-certificated radiologists (D.K.: 10 years of experience; A.Y.: 17 years of experience) in consensus (Fig. 1). The ROI for the hepatic malignant lesions was set as large as possible including the maximum cross-sectional area of the lesion on CTHA and CTAP. The

ROI for the liver parenchyma was set as large as possible avoiding major hepatic vessels such as hepatic arteries, hepatic veins, and portal veins at the same slice as the targeted hepatic malignant lesion on CTHA and CTAP. The ROI for the hepatic artery was set as large as possible including the arterial lumen at the proximal portion of hepatic artery on CTHA. The ROI for the portal vein was set as large as possible including the portal venous lumen at the main trunk of the portal vein on CTAP. As the gold standard for arterial and portal blood flows of the lesion and liver, we calculated the normalized enhancement on CTHA (nCTHA) and on CTAP (nCTAP) of lesions and the liver, respectively. These parameters were calculated as follows:

$nCTAP_{Lesion} = (CTAP_{Lesion} - preconCT_{Lesion}) / (CTAP_{PV} - preconCT_{PV})$

$nCTAP_{Liver} = (CTAP_{Liver} - preconCT_{Liver}) / (CTAP_{PV} - preconCT_{PV})$

$nCTHA_{Lesion} = (CTHA_{Lesion} - preconCT_{Lesion}) / (CTHA_{HA} - preconCT_{HA})$

$nCTHA_{Liver} = (CTAP_{Liver} - preconCT_{Liver}) / (CTAP_{HA} - preconCT_{HA})$

$CTAP_{Lesion}$, $CTAP_{Liver}$, and $CTAP_{PV}$ are the CT values in the lesion, liver, and portal vein on CTAP, respectively. Similarly, $CTHA_{Lesion,}$ $CTHA_{Liver}$, and $CTHA_{HA}$ are the CT values in the lesion, liver, and hepatic artery on CTHA, respectively (Fig. 1A and 1B). The $preconCT_{Lesion}$, $preconCT_{Liver}$, $preconCT_{PV}$, and $preconCT_{HA}$ are the CT values in

the lesion, liver, portal vein, and hepatic artery on pre contrast CT, respectively. The CT value of abdominal aorta was used for approximated $preconCT_{HA}$ to avoid partial volume effect because of small target area on images.

IV-CT protocol

Intravenous multiphasic contrast-enhanced CT including the whole liver was performed using a 64-row CT scanner (Light Speed VCT; GE Healthcare Japan, Tokyo, Japan) at precontrast and 22, 28, 34, 40, 46, 52, 58, 90, and 210 s after the start of an injection of 370 mgI/mL iodine contrast agent (Iopamiron; Bayer Healthcare, Tokyo, Japan) (100 mL) at 3 mL/s through a 22-gauge catheter in the median cubital vein. Scan parameters were as follows: scan range, 25 cm caudal from the upper diaphragm; tube voltage, 120 kVp; tube current, 300 mA (22 s through 58 s, and 210 s) or 500 mA (precontrast and 90 s); matrix, 512 × 512 pixels; field of view, 320 × 320 mm; and reconstruction thickness, 2.5 mm. The median (interquartile range) effective dose was 48.9 mSv (range, 48.2–48.9). This IV-CT protocol was similar to the one described in a previous report [19].

CMA of IV-CT

To analyze the hemodynamics of the liver and various hepatic malignant lesions quantitatively using the CMA of IV-CT, four ROIs were located at the aorta, portal vein, liver, and hepatic malignant lesions manually on the IV-CT images at each contrast-enhanced phase by board-certificated radiologists as mentioned before (D.K.: 10 years of experience; A.Y.: 17 years of experience) in consensus (Fig. 1). The ROI for the hepatic malignant lesions was set as large as possible including the maximum cross-sectional area of the lesion. The ROI for the liver parenchyma was set as large as possible avoiding major hepatic vessels such as hepatic arteries, hepatic veins, and portal veins at the same slice as the targeted hepatic malignant lesion. The ROI for the aorta was set as large as possible including the aortic lumen at the same slice as the targeted hepatic malignant lesion. The ROI for the portal vein was set as large as possible including the portal venous lumen at the main trunk of the portal vein. The contrast-enhanced effects in the ROIs were calculated by subtracting the CT values on postcontrast IV-CT images from the CT values on precontrast images. Because the contrast-enhanced effect and concentration of the iodine contrast medium in the tissue

were linearly correlated, the obtained time-concentration curves (TCCs) were applied into the CMA described by the following differential equation:

$$dC_t(t)/dt = k_{1a}C_a(t - \tau_a) + k_{1p}C_p(t - \tau_p) - k_2C_t(t),$$

where $C_a(t)$, $C_p(t)$, and $C_t(t)$ represent the contrast medium concentrations in the aorta, portal vein, and target tissue (liver or hepatic malignant lesion) at the time $t$. Two inflow rate constants, arterial inflow velocity constant ($k_{1a}$) and portal venous inflow velocity constant ($k_{1p}$), and one outflow velocity constant ($k_2$) were included in the model. $\tau_a$ and $\tau_p$ are the delay parameters representing the physical transit time of the contrast medium from the aorta and portal vein, respectively, to the target tissue.

The differential equation as mentioned before was solved and five perfusion parameters in hepatic malignant lesion and the liver ($k_{1a}$, $k_{1p}$, $k_2$, $\tau_a$, and $\tau_p$) were obtained with the curve-fitting technique using the nonlinear least square method with various parameter limits (Figs. 1E, 1F, and 1G). The calculation was performed five times for each revised upper $k_2$ limit (≦0.01, ≦0.015, ≦0.020, ≦0.025, ≦0.030, ≦0.035, ≦0.040, ≦0.045, ≦0.050, ≦0.060, ≦0.070, ≦0.10, ≦0.50, and ≦1.00) by using MATLAB 2015b (Mathworks, Natick, MA, USA). The lower $k_2$ limit was fixed as zero. The limits for $k_{1a}$ and $k_{1p}$ were not specified ($0 \leqq k_{1a} \leqq 1$, $0 \leqq k_{1p} \leqq 1$).

The Pearson's correlation coefficient between normalized enhancement on IA-CT and perfusion parameters obtained from the CMA of IV-CT ($k_{1a}$ and $k_{1p}$) in lesions and background liver parenchyma was used as a measure of accuracy of the CMA of IV-CT in the evaluation of arterial and portal venous flows. Perfusion parameters were calculated according to various upper $k_2$ limits. The difference in the mean accuracy of CMA of IV-CT according to various upper $k_2$ limits was compared statistically using an analysis of variance (ANOVA) and multiple comparison.

All statistical analysis was performed using MATLAB 2015b (Mathworks). Probability values less than 0.05 were considered statistically significant.

**Results**

The mean correlation coefficient between $k_{1a}$ and nCTHA according to various upper $k_2$ limits was as follows: 0.56 ($k_2$≦0.01), 0.60 ($k_2$≦0.015), 0.62 ($k_2$≦0.02), 0.63 ($k_2$≦0.03), 0.64 ($k_2$≦0.035), 0.65 ($k_2$≦0.04), 0.64 ($k_2$≦0.045), 0.64 ($k_2$≦0.05), 0.64 ($k_2$≦0.055), 0.64 ($k_2$≦0.06), 0.63 ($k_2$≦0.07), 0.61 ($k_2$≦0.1), 0.51 ($k_2$≦0.5), and 0.44 ($k_2$≦1.0). ANOVA revealed that the mean correlation coefficient between $k_{1a}$ and nCTHA differed significantly according to various upper $k_2$ limits ($P < 0.0001$). The

highest mean correlation coefficient was observed when the upper $k_2$ limit was set to between 0.035 ($P < 0.0001$). Multiple comparison revealed that the decrease in correlation coefficient for evaluating arterial blood flow was significant when the upper $k_2$ limit was set to lower than 0.02 or higher than 0.1 compared to the best mean correlation coefficient ($P < 0.05$; Figs. 2 and 3).

The mean correlation coefficient between $k_{1p}$ and nCTAP according to various upper $k_2$ limits was as follows: 0.17 ($k_2 \leqq 0.01$), 0.37 ($k_2 \leqq 0.015$), 0.48 ($k_2 \leqq 0.02$), 0.56 ($k_2 \leqq 0.025$), 0.63 ($k_2 \leqq 0.03$), 0.65 ($k_2 \leqq 0.035$), 0.66 ($k_2 \leqq 0.04$), 0.69 ($k_2 \leqq 0.045$), 0.66 ($k_2 \leqq 0.05$), 0.68 ($k_2 \leqq 0.06$), 0.63 ($k_2 \leqq 0.07$), 0.54 ($k_2 \leqq 0.1$), 0.05 ($k_2 \leqq 0.5$), and 0.09 ($k_2 \leqq 1.0$). ANOVA revealed that the mean correlation coefficient between $k_{1p}$ and nCTAP differed significantly according to various upper $k_2$ limits ($P < 0.0001$). The highest mean concordance rate was observed when the upper $k_2$ limit was set to 0.045 ($P < 0.0001$). Multiple comparison revealed that the decrease in correlation coefficient for evaluating portal venous flow was significant when the upper $k_2$ limit was set to lower than 0.03 or higher than 0.07 compared to the best mean correlation coefficient ($P < 0.05$; Figs. 2 and 4).

The scatter plots of obtained perfusion parameters ($k_{1a}$, $k_{1p}$, and $k_2$) according to hepatic pathology are shown in Fig. 5. Representative cases of HCC, eHCC, and CCC are shown in Figs. 1, 6, and 7, respectively.

**Discussion**

Our results clarified that the accuracy of CMA of IV-CT in the quantitative evaluation of hepatic arterial and portal venous flows can be significantly correlated with that of IA-CT. However, appropriate limits for outflow velocity constant ($k_2$) are mandatory.

Previous studies have reported the usefulness of CMA using IV-CT, because it enables separate and quantitative evaluation of arterial and portal venous blood flows in the liver. Van Beers, et al. and Ronot, et al. reported significant changes in perfusion parameters, especially portal venous flow, among patients with cirrhosis compared to those without cirrhosis using the same compartmental model we used in this study [9,10]. Koh, et al. evaluated arterial and portal perfusion in the liver and HCC by using CMA. They noted that the portal perfusion fraction in the HCC was lower than the normal value, and the HCC appeared hypodense on the portal venous and delayed phases. They concluded that this observation was consistent with the finding that portal perfusion progressively

decreases with increasing de-differentiation of regenerating, dysplastic, and HCC nodules [1-3,15].

However, a direct comparison between the perfusion parameters obtained from the CMA of IV-CT and IA-CT findings, especially in portal venous blood flow, has not been reported before. Miyazaki, et al. reported that hepatic arterial perfusion determined from the CMA of IV-CT was similar to that determined from the CMA of IA-CT, even though portal venous blood flow was not validated using CTAP in their study [20]. Therefore, we believe our study is the first to validate the appropriateness of estimating hepatic portal blood flow via the CMA of IV-CT using CTAP. Our results will have significant clinical relevance in the application of the CMA of IV-CT as a less-invasive substitutional method to IA-CT in liver imaging.

However, non-linear parameter estimation, such as the least square method in curve fitting, is needed to determine the perfusion parameters in the CMA. One of the problems in non-linear parameter estimation is that of a local minima that causes the calculation to converge not at a global optimum solution, but at a local optimum solution. To avoid convergence at the local minima, setting appropriate parameter limits is necessary [18]. However, previous studies have not mentioned taking precautions to

avoid such a situation within the context of a perfusion study. Our results showed that an appropriate evaluation of arterial and portal venous hepatic flows was possible when the upper limit of $k_2$ was set neither too low nor too high. The $k_2$ represents venous out flow during tissue perfusion; therefore, a high $k_2$ correlates with rapid wash out of the contrast medium, resulting in a steep decrease in the TCC between early- and late-phase imaging [16]. Our results showed that the mean correlation coefficient between $k_{1a}$ and nCTHA was relatively good (higher than 0.4) regardless of the $k_2$ limit. In contrast, the mean correlation coefficient between $k_{1p}$ and nCTAP was significantly poor when the upper $k_2$ limit was lower than 0.03 or higher than 0.07. According to these results, the estimation of $k_{1p}$ can be more easily affected by the $k_2$ limit than by the $k_{1a}$. In other words, the local minima problem can have a significant influence on the calculation of $k_{1p}$. When an unreasonably higher $k_2$ value was allowed in the calculation, the TCC of the HCC, which is likely to show more rapid decrease than that of the surrounding liver parenchyma, might be erroneously fitted as the local optimum solution by the TCC of the portal venous vein, resulting in an unreasonably higher $k_{1p}$ than the actual portal venous blood flow in the HCC. However, when only an unreasonably lower $k_2$ value was allowed in the calculation, the TCC of the surrounding liver parenchyma, which is

likely to show a slower decrease than that of the HCC, might be erroneously fitted as the local optimum solution by the TCC of the artery, resulting in an unreasonably lower $k_{1p}$ than the actual portal venous blood flow in the surrounding liver parenchyma.

The clinical relevance of our study is that it will strengthen the reliability of liver perfusion CT study using the CMA for evaluating hepatic hemodynamics, especially in hepatic portal venous flow, as a less-invasive substitutional method to CTAP. Our results will also provide practical and appropriate $k_2$ limits for calculating hepatic perfusion using the CMA. Our findings suggest that the upper $k_2$ limit should be set to between 0.03 and 0.07, because the mean correlation coefficient between the perfusion parameters and IA-CT contrasts are significantly high in both hepatic arterial and portal venous flow evaluation. Furthermore, our results showed that hepatic arterial and portal venous hemodynamics could be evaluated to some extent using CMA even when using relatively low temporal resolution TCC data obtained from IV-CT, compared to the findings of previous studies [9,10,15,20,21] This may imply that the proposed method can be an alternative to an additional dedicated perfusion study, thereby reducing the patient's additional burden and radiation exposure.

This study has some limitations. First, this study was retrospective and the number of

subjects was small especially in histologically proven pathologies other than HCC. However, as shown in representative case presentations, the proposed method could properly discriminate faint portal venous supply of eHCC and prolonged or delayed enhancement of CCC by $k_{1a}$, $k_{1p}$, and $k_2$. Although we did not have a case showing complete delayed enhancement in this study, quantitative classification of hepatic pathologies by CMA of IV-CT may be feasible in future. Second, the biological relevance of the $k_2$ limits is unknown, even though we validated both $k_{1a}$ and $k_{1p}$ using IA-CT. The $k_2$ is also expressed as the inverse of mean transit time, whose usefulness in the evaluation of liver diseases has been reported by several studies [7,9,10,12]. However, a gold standard method to validate $k_2$ is lacking, because it is an apparent value in the calculation of CMA. Further clinical validation of the $k_2$ values obtained using this method is needed in the future.

## Conclusion

In conclusion, hepatic arterial and portal venous flows can be evaluated quantitatively to some extent using appropriate outflow velocity constant limits with the CMA of IV-CT.

Acknowledgments

The authors thank the radiologists and radiographers at our hospital for their cooperation.

**References**

1 Matsui O, Kadoya M, Tomiaki K, et al. Benign and Malignant Nodules in Cirrhotic Livers: Distinction Based on Blood Supply. Radiology. 1991; 178: 493–97.

2 Hayashi M, Mtsui O, Ueda K, et al. Correlation Between the Blood Supply and Grade of Malignancy of Hepatocellular Nodules Associated with Liver Cirrhosis: Evaluation by CT During Intrarateria Injection of Contrast Medium. AJR Am J Roentgenol.1999; 172: 969–72.

3 Hayashi M, Matsui O, Ueda K, Kawamori Y, Gabata T, Kadoya M. Progression to Hypervascular Hepatocellular Carcinoma: Correlation with intranodular Blood Supply Evaluated with CT during Intraarterial Injection of Constant Material. Radiology. 2002; 223: 143–9.

4 Matsui O, Kobayashi S, Sanada J, et al. Hepatocelluar nodules in liver cirrhosis: hemodynamic evaluation (angiography-assisted CT) with special reference to multi-step hepatocarcinogenesis. Abdom Imaging. 2011 Jun; 36: 264–72.

5 Ueda K, Matsui O, Kawamori Y, et al. Hypervascular Hepatocellular Carcinoma: Evaluation of Hemodynamics with Dynamic CT during Hepatic

Arteriography. Radiology. 1998; 206: 161–6.

6 Ash L, Teknos TN, Gandhi D, Patel S, Mukherji SK. Head and Neck Squamous Cell Carcinoma: CT perfusion Can Help Noninvasively Predict Intratumoral Microvessel Density. Radiology. 2009 May; 251: 422–8.

7 Kim JW, Jeong YY, Chang NK, et al. Perfusion CT in colorectal cancer: comparison of perfusion parameters with tumor grade and microvessel density. Korean J Radiol. 2012 Jan-Feb; 13 Suppl 1: S89–97.

8 Kim SH, Kamaya A, Willmann JK. CT perfuison of the Liver: Principles and Applications in Oncology. Radiology. 2014 Aug; 272: 322–44.

9 Van Beers BE, Leconte I, Materne R, Smith AM, Jamart J, Horsmans Y. Hepatic perfusion parameters in chronic liver disease: dynamic CT measurements correlated with disease severity. AJR Am J Roentgenol 2001; 176: 667–73.

10 Ronot M, Asselah T, Paradis V, et al. Liver Fibrosis in Chronic Hepatitis C Virus Infection: Differentiating Minimal from Intermediate Fibrosis with Perfusion CT. Radiology. 2010 Jul; 256: 135–42.

11 Ippolito D, Bonaffini AP, Ratti L, et al. Hepatocellular carcinoma treated with transarterial chemoembolization: Dynamic perfusion-CT in the assessment of residual

tumor. World J Gastroenterol 2010 Dec 21; 16(47): 5993–6000.

12 Taouli B, Johnson RS, Hajdu CH, et al. Hepatocellular carcinoma: perfusion quantification with dynamic contrast-enhanced MRI. AJR Am J Roentgenol. 2013 Oct; 201: 795–800.

13 Kobayashi S, Kitamura A, Matsushita T, Nishiura M, Murase K. Usefulness of a dual-input single-compartment model for quantitative evaluation of thioacetamide-induced acute liver injury in rats using dynamic contrast-enhanced computed tomography. Radiol Phys Technol. 2012 Jan; 5: 27–33.

14 Sourbron S, Sommer WH, Reiser MF, Zech CJ. combined Quantification of liver Perfusion and Function with Dynamic gadoxetic acid– enhanced Mr imaging. Radiology. 2012 Jun; 263: 874–83.

15 Koh TS, Thng CH, Hartono S, et al. Dynamic contrast-enhanced CT imaging of hepatocellular carcinoma in cirrhosis: feasibility of a prolonged dual-phase imaging protocol with tracer kinetics modeling. Eur Radiol. 2009 May; 19: 1184–96.

16 Yamada A. Quantitative Evaluation of Liver Function Within MR Imaging. In: El-Baz A, Saba L, Suri J, eds. Abdomen and Thoracic Imaging. Boston: Springer, 2014; 233–51.

17 Tofts PS. T1-weighted DCE imaging concepts: modelling, acquisition and analysis. Magnetom Flash 2010; 3: 31–9.

18 Local vs. Global Optima. Constrained Optimization. Nonlinear Optimization. Optimization Toolbox: Mathworks Documentation. Available at: https://www.mathworks.com/help/optim/ug/local-vs-global-optima.html. Accessed November 20, 2017.

19 Suzuki T, Yamada A, Komatsu D, et al. Evaluation of splenic perfusion and spleen size using dynamic computed tomography: Usefulness in assessing degree of liver fibrosis. Hepatol Res. 2017 Apr 01.

20 Miyazaki M, Tsushima Y, Miyazaki A, Paudyal B, Amanuma M, Endo K. Quantification of hepatic arterial and portal perfusion with dynamic computed tomography: comparison of maximum-slope and dual-input one-compartment model methods. Jpn J Radiol. 2009 Apr; 27: 143–50.

21 Kanda T, Yoshikawa T, Ohno Y, et al. Hepatic computed tomography perfusion: comparison of maximum slope and dual-input single-compartment methods. Jpn J Radiol. 2010 Dec; 28: 714–9.

Figure legends

Fig. 1. Method of setting the regions of interest

Computed tomography (CT) values in arterial and portal venous input functions, the lesion, and liver are measured as the CT during hepatic arteriography ($CTHA_{HA}$, $CTHA_{Lesion}$, and $CTHA_{Liver}$, respectively; A) and CT during arterioportography ($CTAP_{PV}$, $CTAP_{Lesion}$, and $CTAP_{Liver}$, respectively; B). CT values in the lesion, liver, aorta, and portal vein at scan time t are measured as $C_{t[Lesion]}(t)$, $C_{t[Liver]}(t)$, $C_a(t)$, and $C_p(t)$, respectively, on intravenous multiphasic dynamic contrast-enhanced CT (C: arterial phase and D: portal venous phase). The calculated perfusion parameter maps of classical hepatocellular carcinoma (HCC) and surrounding liver parenchyma (dashed squares in D) are also shown (E: $k_{1a}$, F: $k_{1p}$, and G: $k_2$). Note that increased $k_{1a}$ and $k_2$, and decreased $k_{1p}$ in HCC compared to surrounding liver are quantitatively shown on parameter maps.

Fig. 2. Scatter plots showing the normalized enhancement in computed tomography during hepatic arteriography (CTHA) and the hepatic arterial inflow velocity ($k_{1a}$)

obtained from the compartment model analysis according to various upper limits of the outflow velocity constant (A: $k_2 \leqq 0.01$, B: $k_2 \leqq 0.045$, C: $k_2 \leqq 1$) and scatter plots showing the normalized enhancement in computed tomography during arterioportography (CTAP) and the hepatic portal venous inflow velocity ($k_{1p}$) obtained from the compartment model analysis according to various upper limits of the outflow velocity constant (D: $k_2 \leqq 0.01$, E: $k_2 \leqq 0.045$, F: $k_2 \leqq 1$). Note that correlation between normalized arterial and portal venous enhancements and perfusion parameters change according to various $k_2$ limits.

Fig. 3. The box plot showing the mean correlation coefficients between the normalized enhancement in computed tomography during hepatic arteriography (nCTHA) and hepatic arterial inflow velocity ($k_{1a}$) of the liver and hepatic lesions according to various upper outflow velocity constant ($k_2$) limits. The best mean correlation coefficient of 0.65 is observed when the upper $k_2$ limit is set to 0.035. A significant decrease in concordance rate is observed when the upper $k_2$ limit is set to lower than 0.02 or higher than 0.1.

Fig. 4 The box plot showing the mean correlation coefficients between the normalized enhancement in computed tomography during arterioportography (nCTAP) and the hepatic arterial inflow velocity ($k_{1p}$) of the liver and hepatic lesions according to various upper outflow velocity constant ($k_2$) limits. The best mean correlation coefficient of 0.69 is observed when the upper $k_2$ limit is set to 0.045. A significant decrease in concordance rate is observed when the upper $k_2$ limit is set to lower than 0.03 or higher than 0.07.

Fig. 5 Scatter plots of obtained perfusion parameters (A: $k_{1a}$ vs. $k_2$ B: $k_{1p}$ vs. $k_2$) according to various hepatic pathologies are shown. The upper $k_2$ limit is set to 0.045. Representative cases of HCC (red arrow), eHCC (yellow arrow), and CCC (blue arrow) are shown in Figs. 1, 6, and 7, respectively. Note that the HCC tends to have higher $k_{1a}$ and $k_2$, and lower $k_{1p}$ compared to the other pathologies. eHCC tends to have slightly higher $k_{1a}$ and $k_2$, and slightly lower $k_{1p}$ compared to the surrounding livers. CCC tends to have lower $k_{1a}$, $k_{1p}$, and $k_2$ compared to the other pathologies. Liver: surrounding liver parenchyma, HCC: classical hepatocellular carcionoma, eHCC: early hepatocellular

carcionoma, CoCC: cholangiolocellular carcinoma, mixHCC: mixed hepatocellular carcinoma, CCC: cholangiocellular carcinoma.

Fig. 6 The representative case of early hepatocellular carcinoma (eHCC). The lesion shows slightly increased nodular arterial enhancement on CT during hepatic arteriography (CTHA; A) and slightly decreased portal venous enhancement on CT during arterioportography (CTAP; B). The lesion shows weak nodular enhancement at arterial phase on intravenous-enhancement CT (C); however, 'washout' is not as obvious as that of classical hepatocellular carcinoma (HCC) shown in Fig. 1D at portal venous phase (D). The calculated perfusion parameter maps of eHCC and surrounding liver parenchyma (dashed squares in A, B, C, and D) are also shown (E: $k_{1a}$, F: $k_{1p}$, and G: $k_2$). Note that slightly increased $k_{1a}$ and $k_2$, and slightly decreased $k_{1p}$ in eHCC compared to surrounding liver are quantitatively shown on parameter maps.

Fig. 7 The representative case of cholangiocellular carcinoma (CCC). The lesion shows slightly increased rim-like arterial enhancement on CT during hepatic arteriography (CTHA; A) and decreased portal venous enhancement on CT during arterioportography

(CTAP; B). The left half of lesion is not enhanced on CTHA because of accessory left hepatic artery. The lesion also shows weak rim-like enhancement at arterial phase on intravenous-enhancement CT (C) and progressive central enhancement at portal venous phase (D). The calculated perfusion parameter maps of CCC and surrounding liver parenchyma (dashed squares in A, B, C, and D) are also shown (E: $k_{1a}$, F: $k_{1p}$, G: $k_2$, and H: distribution volume; $V_d = [k_{1a} + k_{1p}]/k_2$). Note that decreased $k_{1a}$, $k_{1p}$, $k_2$ and increased $V_d$ corresponding to progressive arterial enhancement in central part of CCC (*) are quantitatively shown on parameter maps. The distribution volume ($V_d$) is apparent extracellular fluid space volume that contrast media distributes. The progressive arterial enhancement in stroma-rich component of CCC is correctly depicted, instead of erroneously calling it portal venous perfusion.

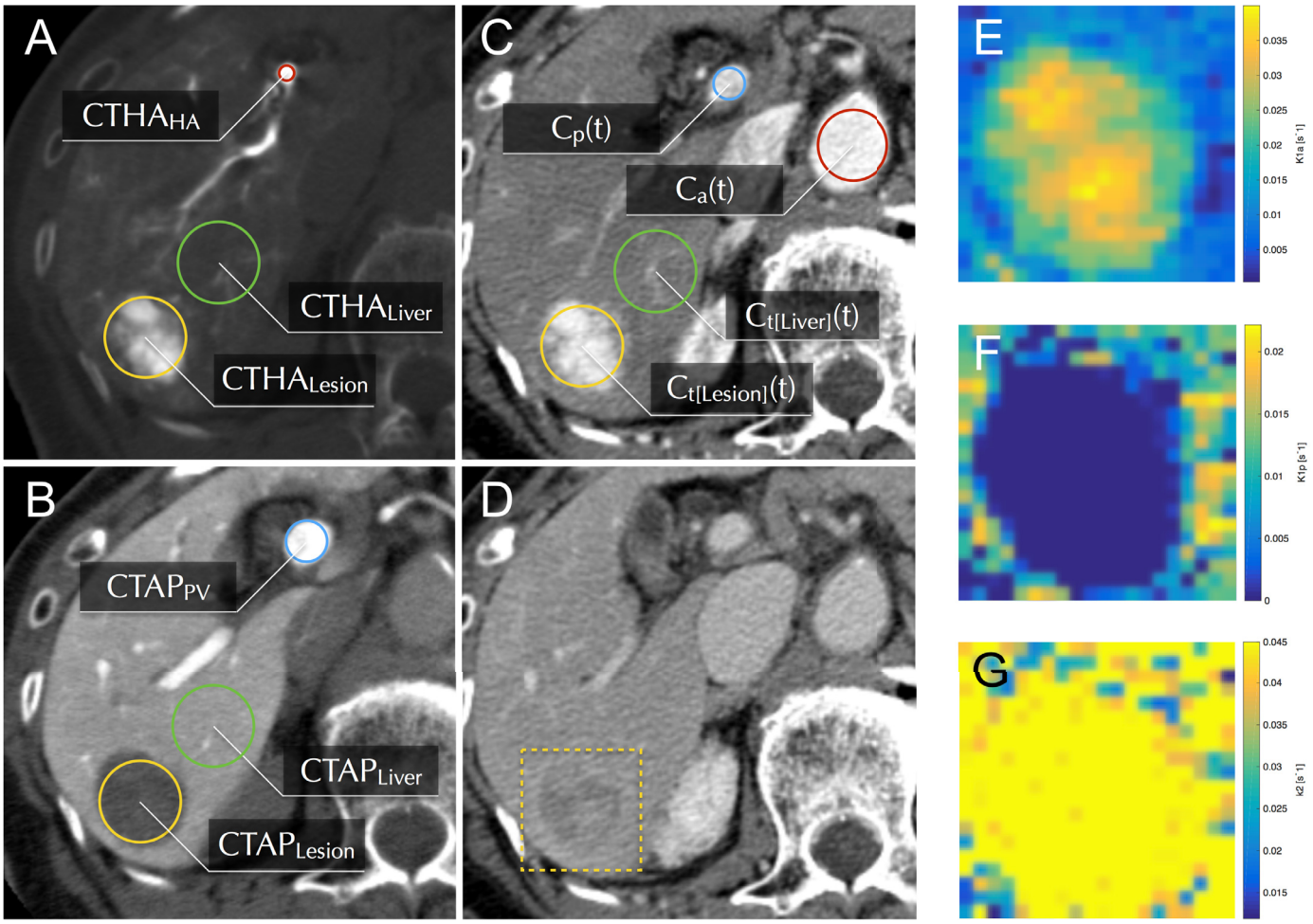
A
CTHA$_{HA}$
CTHA$_{Liver}$
CTHA$_{Lesion}$
B
CTAP$_{PV}$
CTAP$_{Liver}$
CTAP$_{Lesion}$
C
$C_p(t)$
$C_a(t)$
$C_{t[Liver]}(t)$
$C_{t[Lesion]}(t)$
D
E
0.035
0.03
0.025
0.02
0.015
0.01
0.005
K1a [s$^{-1}$]
F
0.02
0.015
0.01
0.005
0
K1p [s$^{-1}$]
G
0.045
0.04
0.035
0.03
0.025
0.02
0.015
k2 [s$^{-1}$]

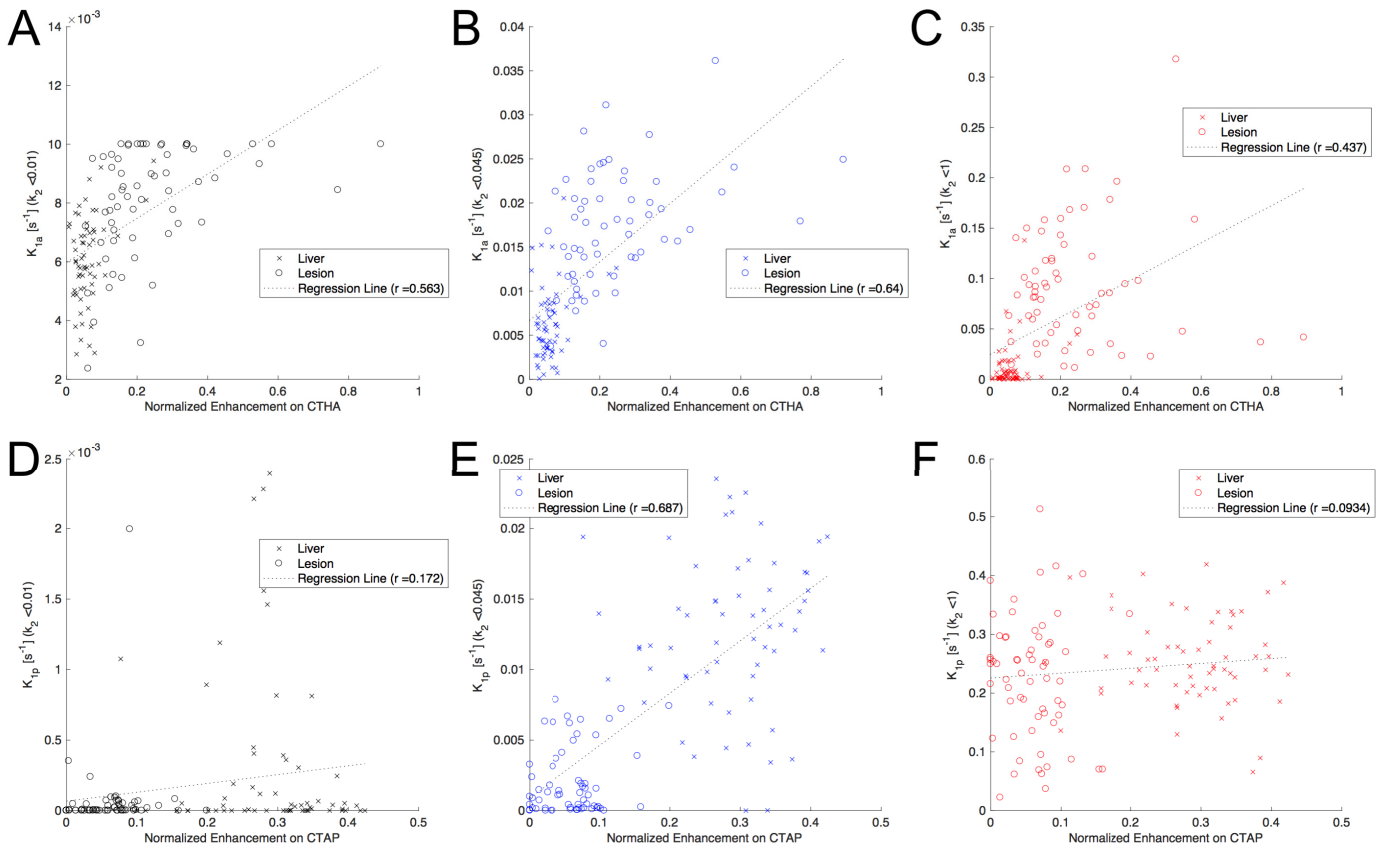
A
B
C
D
E
F
Liver
Lesion
Regression Line (r =0.563)
Regression Line (r =0.64)
Regression Line (r =0.437)
Regression Line (r =0.172)
Regression Line (r =0.687)
Regression Line (r =0.0934)
Normalized Enhancement on CTHA
Normalized Enhancement on CTAP
K1a [s-1] (k2 <0.01)
K1a [s-1] (k2 <0.045)
K1a [s-1] (k2 <1)
K1p [s-1] (k2 <0.01)
K1p [s-1] (k2 <0.045)
K1p [s-1] (k2 <1)

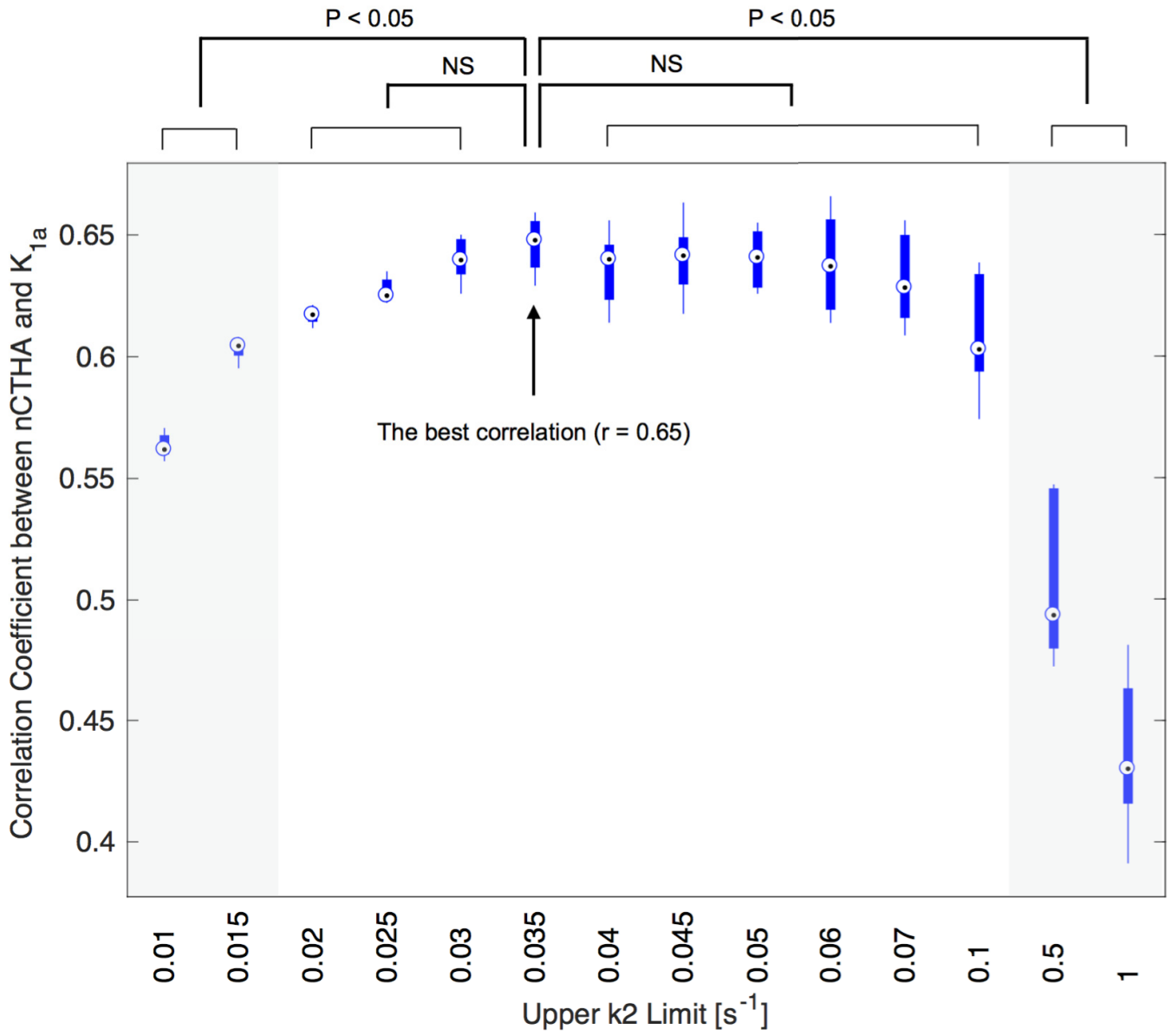
P < 0.05
P < 0.05
NS
NS
Correlation Coefficient between nCTHA and K1a
0.65
0.6
0.55
0.5
0.45
0.4
The best correlation (r = 0.65)
0.01
0.015
0.02
0.025
0.03
0.035
0.04
0.045
0.05
0.06
0.07
0.1
0.5
1
Upper k2 Limit [s-1]

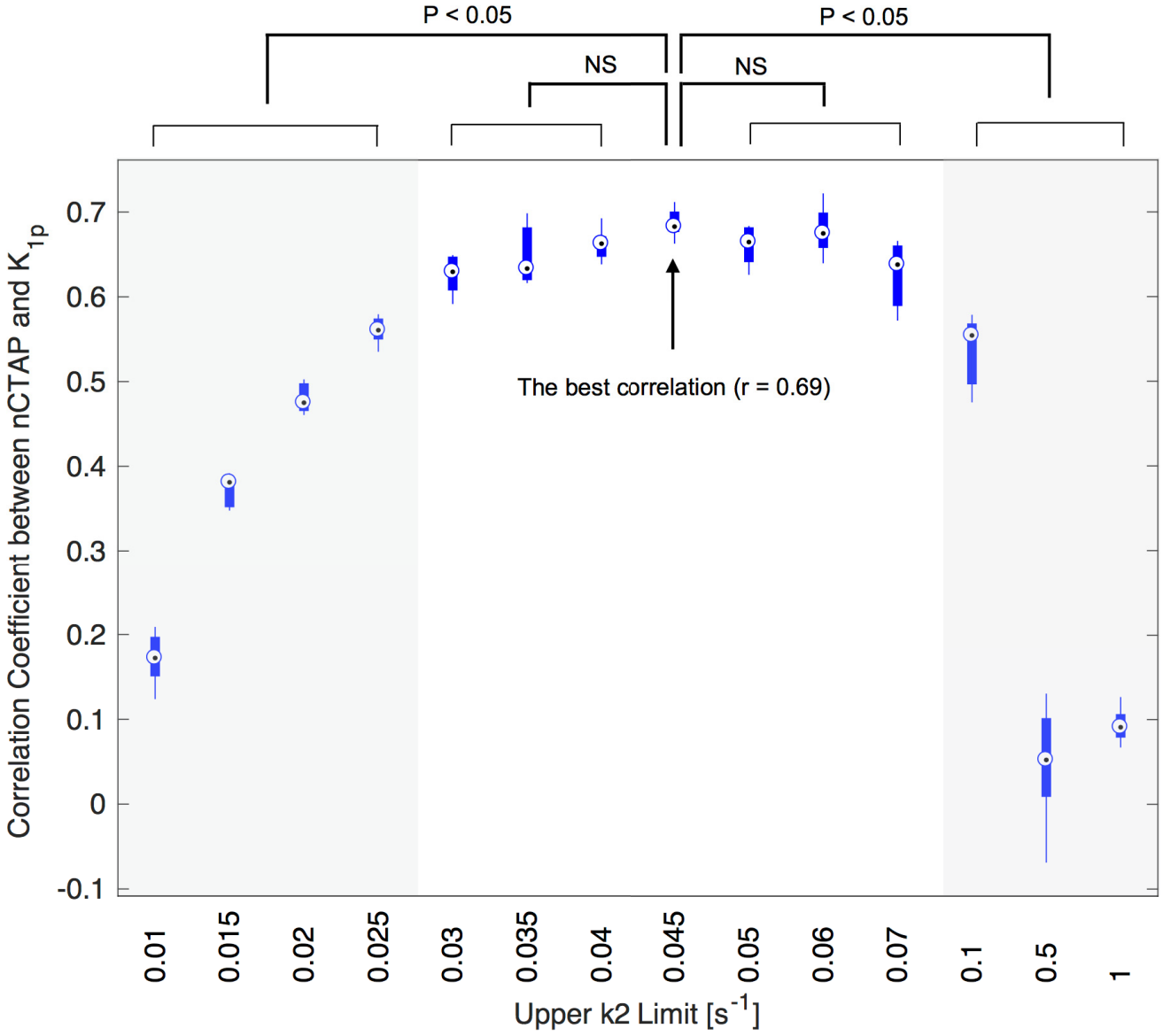
P < 0.05
P < 0.05
NS
NS
The best correlation (r = 0.69)
Correlation Coefficient between nCTAP and K1p
0.7
0.6
0.5
0.4
0.3
0.2
0.1
0
-0.1
0.01
0.015
0.02
0.025
0.03
0.035
0.04
0.045
0.05
0.06
0.07
0.1
0.5
1
Upper k2 Limit [s-1]

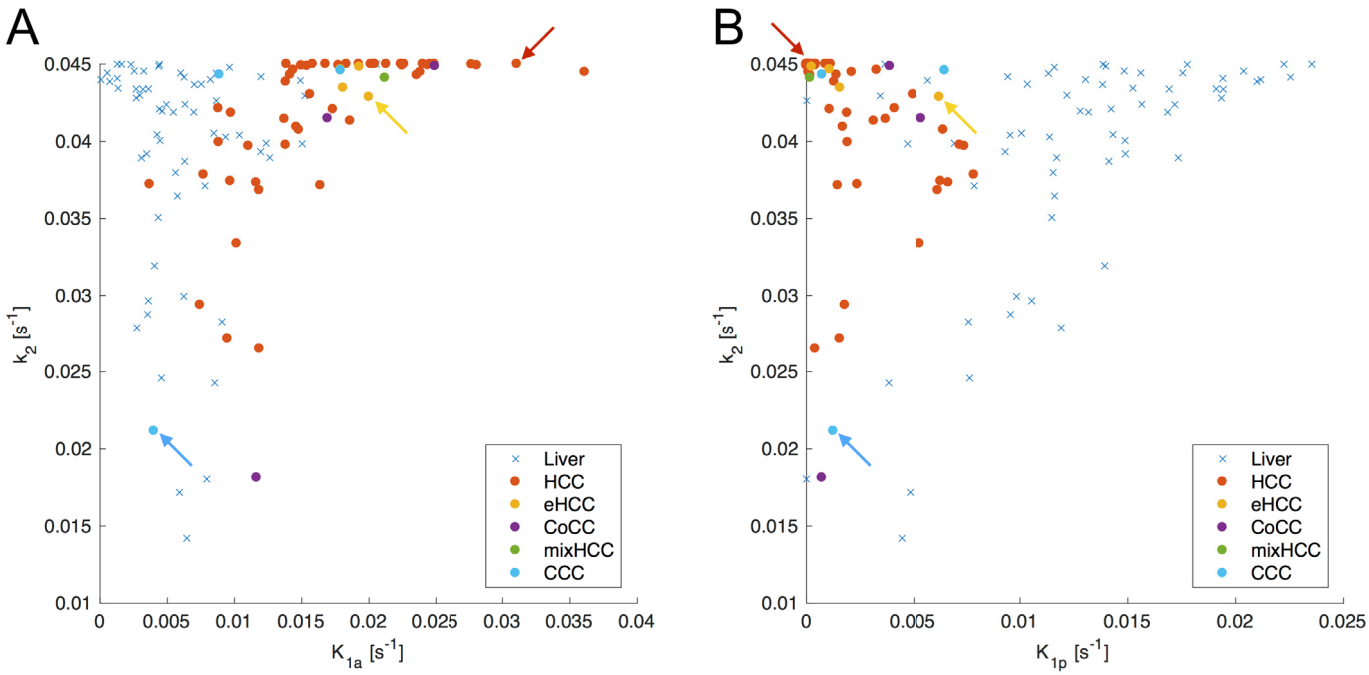
A
B
0.045
0.04
0.035
0.03
0.025
0.02
0.015
0.01
k2 [s-1]
0
0.005
0.01
0.015
0.02
0.025
0.03
0.035
0.04
K1a [s-1]
K1p [s-1]
Liver
HCC
eHCC
CoCC
mixHCC
CCC

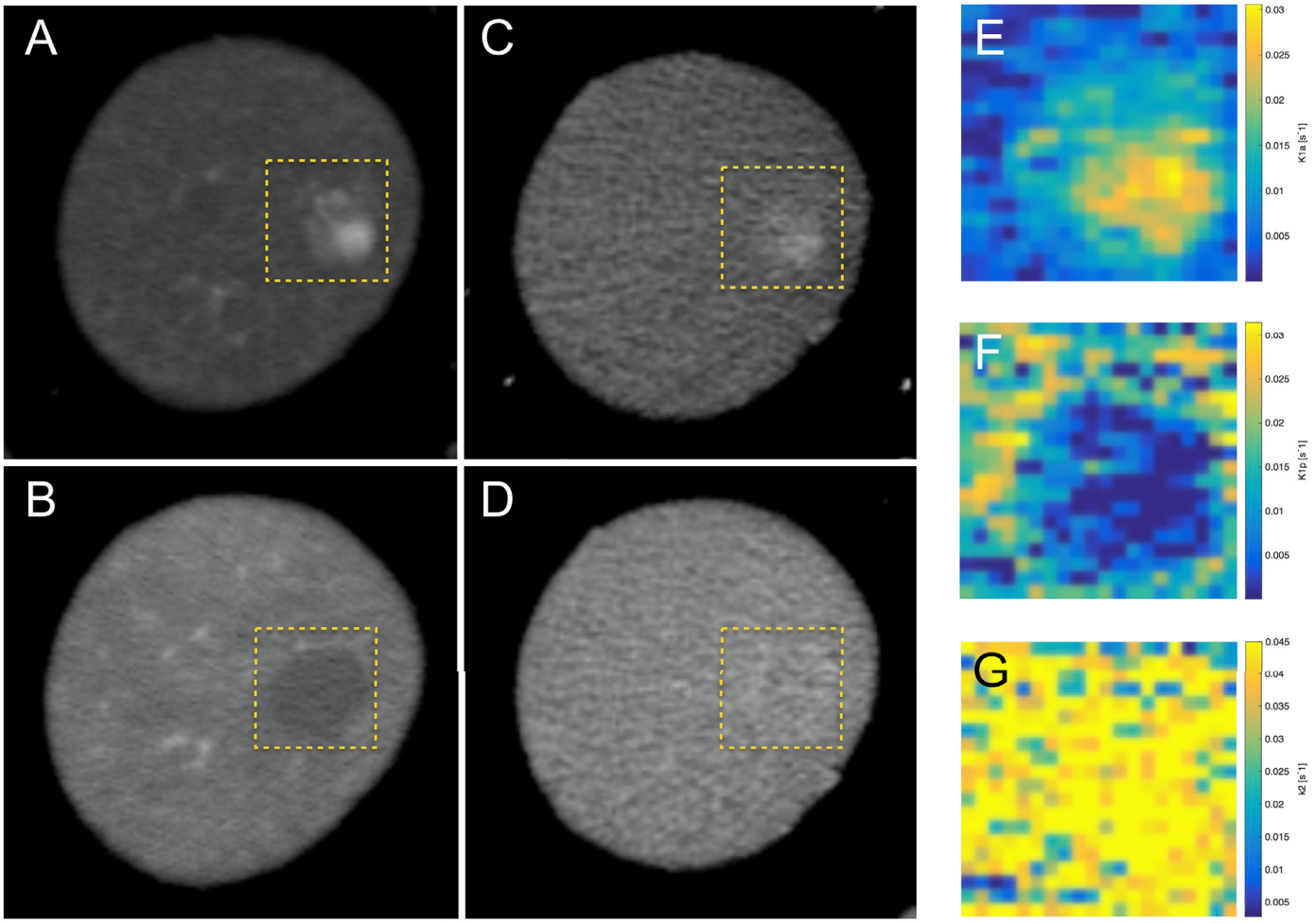
A
C
B
D
E
F
G
0.03
0.025
0.02
0.015
0.01
0.005
K1a [s-1]
K1p [s-1]
0.045
0.04
0.035
0.03
0.025
0.02
0.015
0.01
0.005
k2 [s-1]

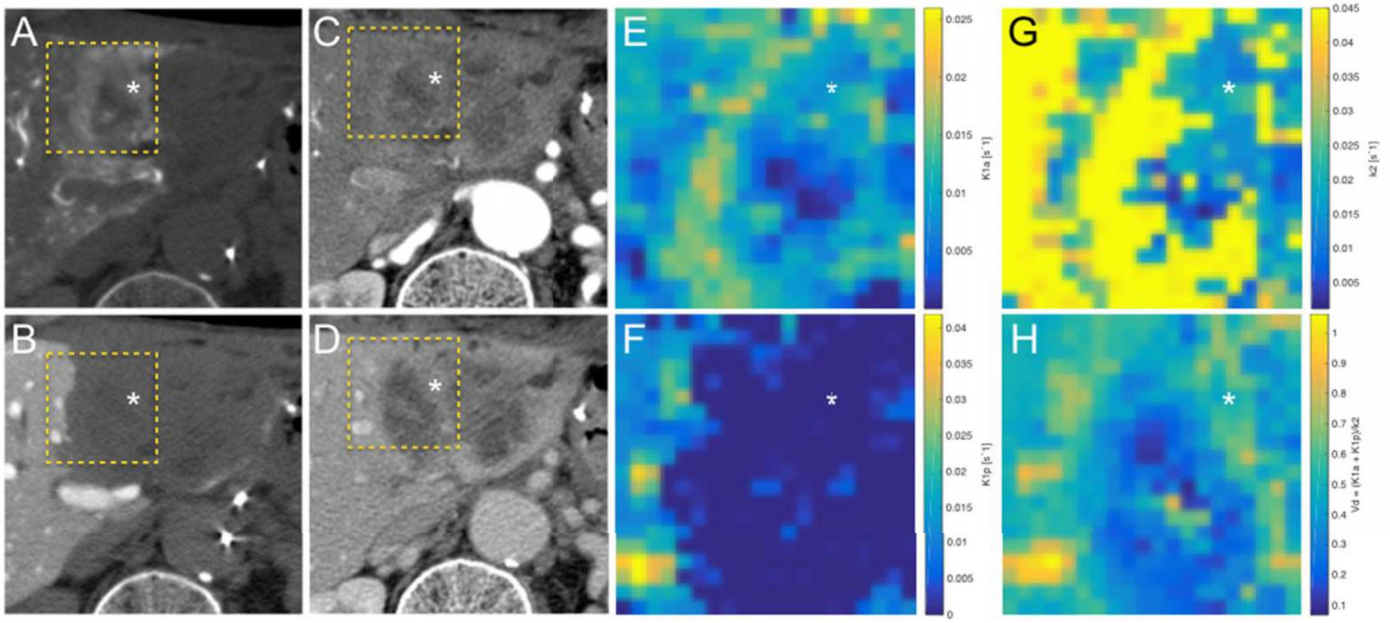
A
B
C
D
E
F
G
H
K1a [s-1]
K1p [s-1]
k2 [s-1]
Vd = (K1a + K1p)/k2